Accurate excluded-volume corrections to the single-chain static properties of a melt of unentangled polymers

2006 J. Phys.: Condens. Matter 18 7543

(http://iopscience.iop.org/0953-8984/18/32/003)

INSTITUTE OF PHYSICS PUBLISHING JOURNAL OF PHYSICS: CONDENSED MATTER

J. Phys.: Condens. Matter **18** (2006) 7543–7552 doi:10.1088/0953-8984/18/32/003

Accurate excluded-volume corrections to the single-chain static properties of a melt of unentangled polymers

D Molin[1], **A Barbieri**[2,3] **and D Leporini**[2,4,5]

[1] Dipartimento di Ingegneria Chimica, Chimica Industriale e Scienza dei Materiali, Universitá di Pisa, via Diotisalvi 1, I-56100 Pisa, Italy
[2] Dipartimento di Fisica 'Enrico Fermi', Università di Pisa, Largo B Pontecorvo 3, I-56127 Pisa, Italy
[3] INFN, Sezione di Pisa, Largo B Pontecorvo 3, I-56127 Pisa, Italy
[4] CNR-INFM-CRS SOFT, Largo B Pontecorvo 3, I-56127 Pisa, Italy

E-mail: dino.leporini@df.unipi.it

Received 13 June 2006
Published 25 July 2006
Online at stacks.iop.org/JPhysCM/18/7543

Abstract

Actual polymer chains cannot cross themselves and each other. However, the popular Rouse model for unentangled polymers considers the chains as being like 'phantoms'. It is shown that excluded volume effects on single-chain statics may be introduced by analytic corrections to the Rouse results. The final expressions do not depend on free parameters. They exhibit excellent agreement with the molecular-dynamics simulations of polymer melts with chain lengths in the range $3 \leqslant M \leqslant 30$. Preliminary results for entangled polymer melts are presented.

1. Introduction

The Rouse model [1] is the simplest bead-spring model for flexible polymer chains [2–4]. Being expressed in terms of either continuous [3] or discrete [5–8] mode distributions, it is usually applied to describe the long-time or large-scale polymer dynamics by neglecting the interactions between monomers which are distant along the chain, i.e. excluded volume, hydrodynamic interactions and chain entanglements are not considered. This model has been frequently applied to non-entangled chains in concentrated solutions. The model also serves in the description of the entangled chains: the tube model analyses the motion of the Rouse chain confined in a tube-like regime for calculating various kinds of dynamic properties [3]. Thus, the Rouse model is one of the most important models in the field of polymer dynamics.

In the Rouse model, each chain is composed of $M_R - 1$ segments being modelled by M_R non-interacting beads, connected by entropic springs with force constant $\kappa = 3k_BT/a_R^2$,

[5] Author to whom any correspondence should be addressed.

where a_R is the average size of the segment (i.e. the root mean square length of the spring), k_B is the Boltzmann constant, and T is the absolute temperature. No other interaction between the beads is present. In particular, this means that the chains are 'phantoms', i.e. they can be crossed by themselves and other chains. The model considers a given chain and regards the surrounding ones as a uniform frictional medium. The surrounding chains are depicted to also exert on each bead of the selected chain a fast-fluctuating random force to ensure proper equilibrium properties via the fluctuation-dissipation theorem. The Rouse model has been tested by experiments [9–12] and numerical simulations [13–19].

The phantom Rouse chains have static properties which differ from the numerical results on more realistic polymer models with excluded volume [17]. It is the purpose of the present paper to discuss how excluded-volume effects may be incorporated into the Rouse theory in terms of analytic corrections. Our approach deals with short, unentangled chains where the usual field-theory renormalization procedure [3, 20] is expected to fail and where, to the best of our knowledge, no effective results are available. Evidence in favour of our treatment is provided by comparing the resulting expressions with molecular-dynamics simulations (MD) performed on a fully flexible polymer model in the range of polymer lengths $3 \leqslant M \leqslant 30$.

The paper is organized as follows. In section 2, the excluded-volume corrections are derived. In section 3, the numerical methods are presented. In section 4, the theoretical results are compared with the simulations.

2. Excluded-volume corrections

The discrete [5, 8] Rouse model [1] describes a single linear chain as a series of $M_R - 1$ segments being modelled by M_R non-interacting beads, connected by entropic springs in the presence of a highly damping Gaussian environment. The solution, i.e. the position of the nth bead $\mathbf{r}_n$, is conveniently expressed in terms of normal coordinates, the so-called Rouse modes $\mathbf{X}_p^R$ with $p = 0, \ldots, M_R - 1$, to be written as:

$$\mathbf{X}_p^R(t) = \frac{1}{M_R} \sum_{n=1}^{M_R} \mathbf{r}_n(t) \cos\left[\frac{(n-1/2)p\pi}{M_R}\right]. \tag{1}$$

Henceforth, the mode with index $p = 0$, i.e. the chain centre-of-mass, will not be considered. The static cross-correlations between the Rouse modes vanish. In particular, for $p, q > 0$,

$$\langle \mathbf{X}_p^R \cdot \mathbf{X}_q^R \rangle = \delta_{pq} \frac{a_R^2}{8M_R \sin^2(p\pi/2M_R)}. \tag{2}$$

The Rouse chain provides a coarse-grained picture of flexible linear polymers with bond length b_0 and M monomers, the mth one being located at the position $\mathbf{R}_m$, $1 \leqslant m \leqslant M$. The segment and the bond lengths are related via the characteristic ratio C_∞ by $a_R = \sqrt{C_\infty} b_0$ [3]. The rationale is that the presence of excluded volume results in a homogeneous dilation of the chain at the largest length scales [20]. For fully flexible chains, $\sqrt{C_\infty} \sim 1$ [17, 21] and the identification $M_R = M$ is safe. In that case, the actual route to calculate the modes in numerical simulations starts by defining ($1 \leqslant p \leqslant M - 1$):

$$\mathbf{X}_p(t) = b_0 \sum_{n=1}^{M-1} d_{pn} \mathbf{b}_n(t) \tag{3}$$

where $\mathbf{b}_m$ is the unit vector along the mth bond of the chain:

$$\mathbf{b}_m = \frac{1}{b_0}(\mathbf{R}_{m+1} - \mathbf{R}_m) \tag{4}$$

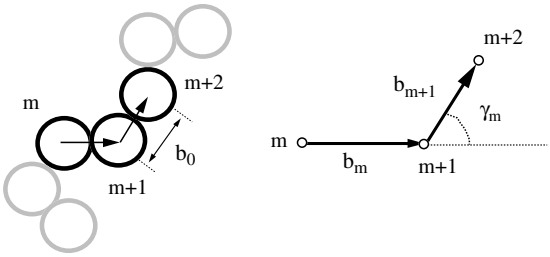

Figure 1. (Left) The polymer model under study: a fully flexible linear chain with M monomers pictured as soft or hard spheres and fixed bond length b_0. The portion between the mth monomer and the $(m+2)$th monomer is emphasized. (Right) The definition of the bond (or valence) angle γ_m between the mth bond and the $(m+1)$th bond.

and

$$d_{pn} = -\frac{1}{2M} \sin\left[\frac{pn\pi}{M}\right] \mathrm{cosec}\left[\frac{p\pi}{2M}\right]. \tag{5}$$

The static cross-correlations between the modes read:

$$\langle \mathbf{X}_p \cdot \mathbf{X}_q \rangle = \delta_{pq} \frac{b_0^2}{8M \sin^2(p\pi/2M)} + b_0^2 \sum_{i=1}^{M-2} D_{pqi} \tag{6}$$

with

$$D_{pqi} = \sum_{k=1}^{M-1-i} (d_{pi} d_{qi+k} + d_{qi} d_{pi+k}) \langle \mathbf{b}_i \cdot \mathbf{b}_{i+k} \rangle. \tag{7}$$

The first term on the right-hand side (rhs) of equation (6) coincides with equation (2) having replaced the mean square length of the Rouse segment a_R^2 with the square length of the bond b_0^2 and the number of Rouse segments with the number of bonds. The second term of equation (6) provides the corrections due to the non-vanishing static correlations between different bonds. If the chain is a phantom, then $\langle \mathbf{b}_m \cdot \mathbf{b}_{m+k} \rangle = \delta_{k0}$ and the corrections vanish, i.e. $D_{pqi} = 0$.

2.1. Bond–bond static correlations

Equations (6) and (7) show that the static properties of the Rouse modes with $p > 0$ depend on the bond–bond static correlation $\langle \mathbf{b}_m \cdot \mathbf{b}_{m+k} \rangle$, i.e. the average cosine of the angle between the mth and $(m+k)$th bonds. Explicit expressions of the latter quantity have been known for a long time for the case of linear chains with a *fixed* bond (or valence) angle $\gamma_m = \gamma$ between the mth and $(m+1)$th bonds (see figure 1, right) both in the absence [22] and the presence [23] of a torsional potential $U(\phi_m)$, where ϕ_m is the dihedral angle, hindering the rotation of the chain around the mth bond. These results were reviewed by Flory [24] and, more recently, by others [3, 25].

Here, we are interested in a variant of the above well-known results which, to the best of our knowledge, has not been discussed earlier, i.e. the possibility that the valence angle γ_m is *not* fixed and spans a finite range, being limited by the excluded volume effects between the mth and the $(m+2)$th beads. Analogously to the classical treatments of the case with fixed valence angle [3, 24, 25], the statistics of both the valence and the dihedral angles are taken as being independent of each other and also independent of the bond position m along the chain. For the present purposes, torsional potentials are neglected, i.e. the dihedral angle ϕ covers the range $0 \leqslant \phi \leqslant 2\pi$ with equal probability.

First, the scalar product $\mathbf{b}_m \cdot \mathbf{b}_{m+k}$ is considered. With this aim, a local coordinate system is introduced for each of the bonds. For the mth bond, one takes the x_m axis along the mth bond, whereas the y_m axis lies in the plane formed by the bonds m and $m-1$ so that the angle between the axes x_{m-1} and y_m is acute. The z_m axis is directed so as to make the cartesian coordinate system right-handed. To proceed, the vector $\mathbf{b}_{m+k}$ is transformed by successive transitions from its own coordinate system to the coordinate system of the mth bond (from the $(m+k)$th to the $(m+k-1)$th bond, then from the $(m+k-1)$th to the $(m+k-2)$th bond, and so on). In this system, the vector $\mathbf{b}_{m+k}$ reads[6]

$$\mathbf{b}'_{m+k} = \mathbf{T}_m \mathbf{T}_{m+1} \dots \mathbf{T}_{m+k-1} \mathbf{b}_{m+k} \tag{8}$$

where the $\mathbf{T}_m$ matrix transforms the $(m+1)$th coordinate system to the mth one:

$$\mathbf{T}_m = \begin{pmatrix} \cos\gamma_m & \sin\gamma_m & 0 \\ \sin\gamma_m \cos\phi_m & -\cos\gamma_m \cos\phi_m & \sin\phi_m \\ \sin\gamma_m \sin\phi_m & -\cos\gamma_m \sin\phi_m & -\cos\phi_m \end{pmatrix}. \tag{9}$$

Then

$$\mathbf{b}_m \cdot \mathbf{b}_{m+k} = \{\mathbf{T}_m \mathbf{T}_{m+1} \dots \mathbf{T}_{m+k-1}\}_{11} \tag{10}$$

where $\{\mathbf{X}\}_{ij}$ denotes the ij element of the $\mathbf{X}$ matrix. The average $\langle \mathbf{b}_m \cdot \mathbf{b}_{m+k} \rangle$ is expressed as

$$\langle \mathbf{b}_m \cdot \mathbf{b}_{m+k} \rangle = \{\langle \mathbf{T}_m \mathbf{T}_{m+1} \dots \mathbf{T}_{m+k-1} \rangle\}_{11} \tag{11}$$

$$= \{\langle \mathbf{T} \rangle^k\}_{11} \tag{12}$$

with

$$\langle \mathbf{T} \rangle = \begin{pmatrix} \langle \cos\gamma \rangle & \langle \sin\gamma \rangle & 0 \\ 0 & 0 & 0 \\ 0 & 0 & 0 \end{pmatrix} \tag{13}$$

which yields:

$$\langle \mathbf{b}_m \cdot \mathbf{b}_{m+k} \rangle = \langle \cos\gamma \rangle^{|k|}. \tag{14}$$

We are now in a position to include the excluded-volume effects into the model. We present two different models: (*i*) hard monomers (HM); (*ii*) soft monomers (SM).

2.1.1. Hard monomers. For a fully flexible linear chain of monomers pictured as hard spheres with diameter σ, linked to each other by bonds with length b_0 (see figure 1, left), the valence angle γ spans the range $0 \leqslant \gamma \leqslant \gamma_{\max}$, where $\gamma_{\max} = \pi - 2\arcsin(\sigma/2b_0)$. One finds:

$$\langle \cos\gamma \rangle^{(\mathrm{HM})} = \frac{1}{1-\cos\gamma_{\max}} \int_{\cos\gamma_{\max}}^{1} x \, \mathrm{d}x \tag{15}$$

$$= \cos^2\left(\frac{\gamma_{\max}}{2}\right) \tag{16}$$

$$= \left(\frac{\sigma}{2b_0}\right)^2. \tag{17}$$

From equation (14), one has

$$\langle \mathbf{b}_m \cdot \mathbf{b}_{m+k} \rangle^{(\mathrm{HM})} = \left(\frac{\sigma}{2b_0}\right)^{2|k|}. \tag{18}$$

Usually, $b_0 \sim \sigma$, i.e. $\gamma_{\max} \sim 120°$, and then $\langle \mathbf{b}_m \cdot \mathbf{b}_{m+k} \rangle$ is negligible for $k > 2$.

[6] Equations (8)–(12) are taken from [25], pp 12–13, after having amended some misprints.

2.1.2. Soft monomers. Now let us consider a fully flexible linear chain with bond length b_0 and non-bonded monomers interacting via the Lennard-Jones (LJ) potential $U(r)$:

$$U(r) = 4\epsilon\left[(\sigma/r)^{12} - (\sigma/r)^{6}\right]. \tag{19}$$

As a first step, the canonical average $\langle\cos\gamma\rangle$ was evaluated as:

$$\langle\cos\gamma\rangle^{(\mathrm{SM0})} = \frac{\int_0^{2b_0}\left(\frac{r^2}{2b_0^2} - 1\right) r\mathrm{e}^{-\beta U(r)}\,\mathrm{d}r}{\int_0^{2b_0} r\mathrm{e}^{-\beta U(r)}\,\mathrm{d}r}. \tag{20}$$

Later, it will be shown that the above expression leads to some, but not remarkable, agreement with the numerical simulations, in that it overestimates the role of the attractive tail of the LJ potential. In fact, the Weeks–Chandler–Andersen reference-potential theory (WCA) proves that the static properties of dense monatomic liquids may be effectively calculated by treating the attractive part of the potential as a perturbation on a hard-sphere system [26]. In practice, WCA divides the potential $U(r)$ into a reference potential $U_0(r)$ and considers the difference $U(r) - U_0(r)$ as a small perturbation. In particular, WCA shows that the static properties of the reference fluid, i.e. the one with interactions governed by $U_0(r)$, may be mapped into the properties of a fluid of hard spheres with an effective diameter σ^{WCA}. In the present case, the reference potential takes the form of the truncated Lennard-Jones potential:

$$U_{\mathrm{T}}(r) = (U(r) + 1)H(\sqrt[6]{2}\,\sigma - r) \tag{21}$$

where $H(x)$ is the Heaviside step function. $U_{\mathrm{T}}(r)$ vanishes in the minimum of $U(r)$ and ensures that the force is continuous.

The WCA theory deals with monatomic liquids and, therefore, does not provide routes to evaluate the average $\langle\cos\gamma\rangle$. No hints are also given by PRISM theory, a recent extension of WCA to polymers, where the focus is on the interchain correlations and the intrachain static structure, of interest here, is needed as input information [27].

As a first guess we modified equation (17) as

$$\langle\cos\gamma\rangle^{(\mathrm{SM1})} = \left(\frac{\sigma^{\mathrm{WCA}}}{2b_0}\right)^2 \tag{22}$$

where σ^{WCA} was evaluated according to standard iterative procedures [26, 28]. However, the above equation differs little from equation (17), since we found $\sigma^{\mathrm{WCA}}/\sigma \sim 1.01$, in agreement with others [28]. Equation (17) disagrees with numerical simulations of polymer chains with soft monomers (see later). As an alternative, we evaluated the average $\langle\cos\gamma\rangle$ as a canonical average by using $U_{\mathrm{T}}(r)$ in the Boltzmann weight:

$$\langle\cos\gamma\rangle^{(\mathrm{SM2})} = \frac{\int_0^{2b_0}\left(\frac{r^2}{2b_0^2} - 1\right) r\mathrm{e}^{-\beta U_{\mathrm{T}}(r)}\,\mathrm{d}r}{\int_0^{2b_0} r\mathrm{e}^{-\beta U_{\mathrm{T}}(r)}\,\mathrm{d}r}. \tag{23}$$

However, the above approximation also led to values differing little from equation (17). In contrast to equation (20), both equations (22) and (23) underestimate the attractive tail of the LJ potential. Having noted that the *full* inclusion of the attractive tail of the LJ potential in the SM0 model leads to some agreement with the numerical simulations, we finally tried the following *ansatz*:

$$\langle\cos\gamma\rangle^{(\mathrm{SM3})} = \frac{\int_0^{2b_0}\left(\frac{r^2}{2b_0^2} - 1\right) \mathrm{e}^{-\beta U_{\mathrm{T}}(r)}\,\mathrm{d}r}{\int_0^{2b_0} \mathrm{e}^{-\beta U_{\mathrm{T}}(r)}\,\mathrm{d}r}. \tag{24}$$

The ansatz increases the weight of configurations with close monomers (small r values). Notice that $\langle\cos\gamma\rangle^{(\mathrm{SM3})}$ is about 25% smaller than $\langle\cos\gamma\rangle^{(\mathrm{SM2})}$. Below, it will be shown that the above

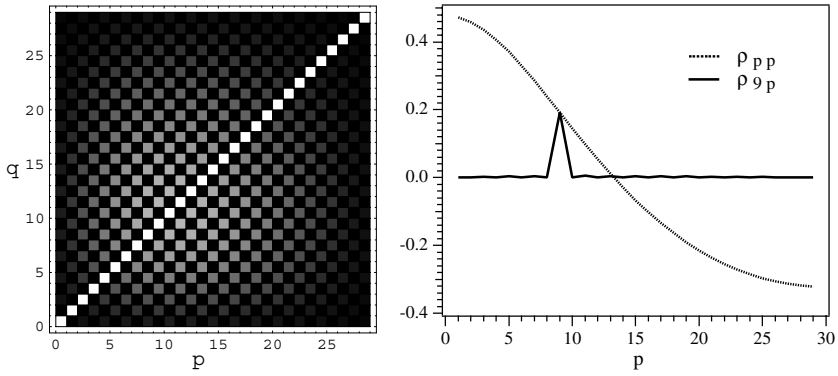

Figure 2. Left: density plot of $|\rho_{pq}|$ being evaluated by the SM3 model with $M = 30$, $b_0 = 0.97$, and $k_B T/\epsilon = 1.2$. Lighter squares correspond to higher values; black squares mean $\rho_{pq} = 0$. Right: selected sections of ρ_{pq}.

ansatz is quite effective. Henceforth, for comparison purposes we define, via equation (14), the following form:

$$\langle \mathbf{b}_m \cdot \mathbf{b}_{m+k} \rangle^{(\mathrm{SM}i)} = \left[\langle \cos\gamma \rangle^{(\mathrm{SM}i)} \right]^{|k|}, \qquad i = 0, \ldots, 3. \tag{25}$$

2.2. Magnitude of the excluded-volume corrections

To assess how large the excluded-volume corrections with respect to the Rouse original results for phantom chains are, it is useful to consider the ratio

$$\rho_{pq} = \frac{\sum_{i=1}^{M-2} D_{pqi}}{\sqrt{\frac{1}{8M\sin^2(p\pi/2M)}}\sqrt{\frac{1}{8M\sin^2(q\pi/2M)}}}. \tag{26}$$

Equation (25) for the SM3 model allows one to evaluate explicitly the above quantity. Figure 2 (left) shows a semi-qualitative plot of ρ_{pq} for $M = 30$. It is found that the excluded-volume effects do largely affect the moduli of the modes, whereas their orthogonality breaks down weakly. Irrespective of the excluded-volume corrections, it is also seen that the matrix element $\langle \mathbf{X}_p \cdot \mathbf{X}_q \rangle$ still vanishes if the pair (p, q) is made by odd–even pairs of numbers. Figure 2 (right) shows selected cross sections of ρ_{pq}.

3. Numerical methods

We investigate systems of N fully flexible linear chains with M monomers using molecular-dynamics methods (MD). The (M, N) pairs under investigation are $(3, 667)$, $(5, 200)$, $(10, 200)$, $(15, 220)$, $(22, 300)$ and $(30, 300)$. The interaction between non-bonded monomers occurs via the Lennard-Jones (LJ) potential, equation (19). Actually, the potential is cut off at $r_{\mathrm{cut}} = 2.5\sigma$ and properly shifted so as to vanish at that point and to make it continuous everywhere. The *RATTLE* [29] algorithm is used to constrain neighbouring monomers in the same chain at distance $b_0 = 0.97\sigma$. From now on, LJ units are adopted with the Boltzmann constant $k_B = 1$. The samples are equilibrated under Nosé–Andersen [29] dynamics at a given temperature and pressure. Data are collected during production runs in microcanonical conditions. Further details are given elsewhere [21]. The system is studied at the constant pressure $P = 2.0$ and temperature $T = 1.2$ corresponding to number densities in the range

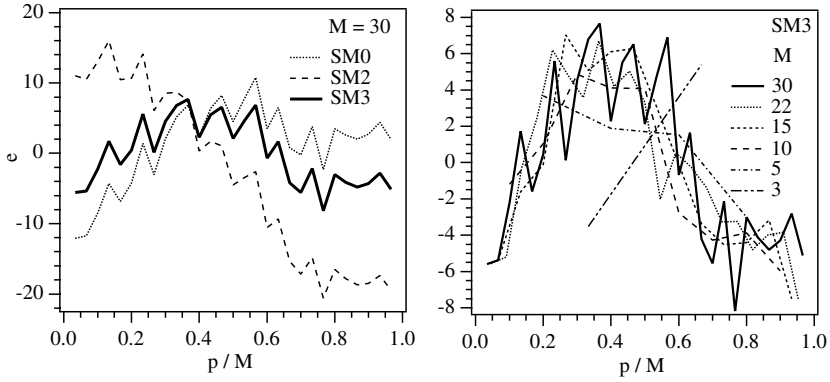

Figure 3. Relative error $e = 10^2 \times (\langle|\mathbf{X}_p|^2\rangle^{(\mathrm{SM}i)}/\langle|\mathbf{X}_p|^2\rangle - 1)$ between MD data and the SM0, SM2 and SM3 models for $M = 30$ (left) and the SM3 model for all the molecular weights under investigation (right). No free parameters. The deviations of HM, SM1 and SM2 models are quite similar and, for clarity reasons, only the latter is shown.

$0.91 \leqslant \rho \leqslant 0.95$. The results have been averaged over at least ten independent runs. Note that the present range of chain lengths is below the entanglement length of the present model $N_\mathrm{e} \sim 32$ [19].

4. Results and discussion

The modes $\mathbf{X}_p$ are found to be fairly orthogonal. In fact, the quantity $\langle \mathbf{X}_p \cdot \mathbf{X}_q \rangle$ with $p \neq q$ is two to three orders of magnitude less than the moduli of the involved modes (data not shown). Moreover, the temperature dependence of the moduli of the Rouse modes was found to be negligible in the range $0.65 \leqslant T \leqslant 1.8$ for $M = 10$ (data not shown). Both findings are in agreement with other studies [15, 17].

Figure 3 plots the relative errors between the MD simulations and the predictions of the SMi models via equation (6) in terms of the reduced index p/M. No parameters were adjusted. The left panel shows that, for $M = 30$, the SM3 model agrees better than the other SMi and HM models. The right panel shows that, apart from the trimer case ($M = 3$), the deviations of the SM3 model for the other chain lengths are fairly superimposed on each other within the statistical errors. This is a consequence of the good scaling with respect to the reduced index p/M of the moduli from both the MD data (see below) and the SMi model (one notes by inspection that $\langle|\mathbf{X}_p|^2\rangle^{(\mathrm{SM}i)} \cong M^{-1}\phi'(p/M)$).

Further insight into the SM3 model is provided by figure 4, which plots the moduli of the modes for all the chain lengths under study and compares the numerical results with equation (6). It is seen that the model ensures good agreement with MD data over a range of the moduli spanning more than two orders of magnitude. The left panel of figure 4 analyses the case with $M = 10$ in detail. It is seen that the Rouse model with the identification $a_\mathrm{R} = b_0$ does not work. Assuming homogeneous dilation, i.e. setting $a_\mathrm{R} = \sqrt{C_\infty} b_0$ [3, 20], improves the comparison, but for the modes with low-p index only. These findings are known [17] and are anticipated, in that the homogeneous-dilation picture follows by a renormalization procedure, keeping the structural details at the largest length scales only [20]. The latter are just accounted for by the Rouse modes with a low-p index [3]. Figure 4 (left) also shows that the HM model (similarly to the SM1 and SM2 models) corrects the Rouse model too much, i.e. it overestimates the excluded-volume effects, whereas good agreement is provided by the SM3 model for all

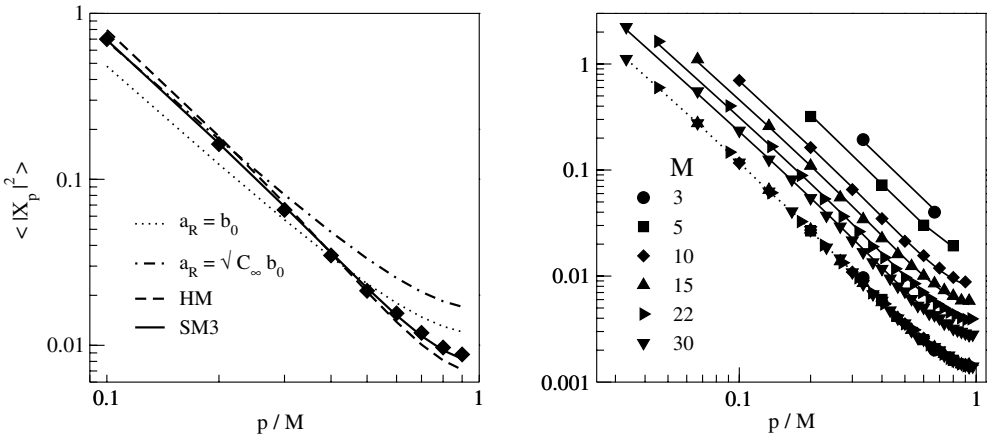

Figure 4. The moduli of the modes $\mathbf{X}_p$ (equation (3)) for different chain lengths M and $1 \leqslant p \leqslant M-1$. Left: comparison between different models and the MD simulation with $M = 10$. The dotted and the dot–dashed lines are the predictions of the Rouse model (equation (2)) by taking the segment length a_R equal to the bond length and assuming homogeneous dilation of the bond length [3, 20], respectively. Both the HM and SM3 models have no adjustable parameters. Right: comparison of the SM3 model (continuous lines) with all the MD data. No parameters were adjusted. The lowest curve is the plot of $\langle|\mathbf{X}_p|^2\rangle$ for all the chain lengths, having shifted the curves vertically by the quantity $\log(C/M)$, with C being a constant. The dotted line is a guide for the eye.

the modes, i.e. for *all* the relevant length scales. Figure 4 (right) validates the SM3 model also for all the polymer lengths under study with *no adjustable* parameters. Figure 4 (right) shows that $\langle|\mathbf{X}_p|^2\rangle \cong M^{-1}\phi(p/M)$, i.e. it scales with respect to the reduced index p/M. That scaling is predicted by the Rouse model (see equation (2)) but it cannot be anticipated on more general grounds. In general, $\mathbf{X}_p$ accounts for the local structure and motion of chains with M/p bonds [3]. The observed scaling proves that, irrespective of the chain length M, portions of the overall chain with the same number of bonds exhibit very similar structures in the range $3 \leqslant M \leqslant 30$. That finding suggests that cross-correlations between bonds which are far apart along the chain are weak. In fact, neglecting completely the cross-correlations, i.e. setting $\langle \mathbf{b}_m \cdot \mathbf{b}_{m+k}\rangle = \delta_{k0}$, leads to phantom Gaussian chains which exhibit the same scaling.

One may wonder whether the elementary models discussed here apply to longer, *entangled* chains as well. A thorough analysis goes beyond the purposes of the present paper. However, a preliminary result is obtained by considering the available MD data on the first Rouse modes of a dense melt of chains each consisting of M freely jointed tangent ($b_0 = \sigma$) hard spheres [30]. The authors consider that, for a *continuous* model, the Rouse mode $\mathbf{X}_p$ is defined as [3]:

$$\mathbf{X}_p = \frac{1}{M}\int_0^M \mathrm{d}n \cos\left(\frac{p\pi n}{M}\right)\mathbf{R}_n. \tag{27}$$

They approximate the above integral by using a trapezoidal integration and write

$$\mathbf{X}_p = \frac{1}{M}\left\{\sum_{n=1}^{M}\left[\mathbf{R}_n \cos\left(\frac{p\pi(n-1)}{M-1}\right)\right] - \frac{1}{2}[\mathbf{R}_1 + (-1)^p\,\mathbf{R}_M]\right\}. \tag{28}$$

Equation (28) corrects a misprint with respect to the original equation (16) of [30]. For the sake of correctness, it must be noted that the latter has another problem (also present in equation (28)), since the trapezoidal integration does not express the leftmost factor as M^{-1} but as $(M-1)^{-1}$. Nonetheless, for the purpose of comparing our HM model with the

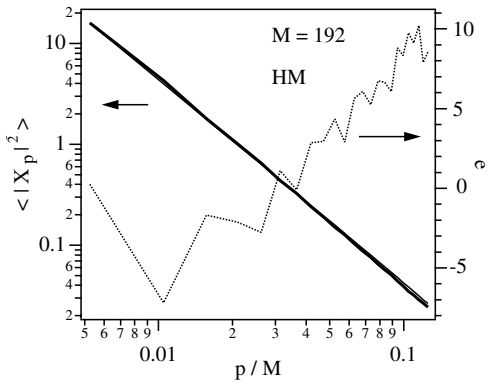

Figure 5. Comparison between the HM model and the modulus of the first Rouse modes of chains, each consisting of M freely jointed tangent hard spheres ($M = 192$) [30]. The relative error $e = 10^2 \times (\langle|\mathbf{X}_p|^2\rangle^{(\mathrm{HM})}/\langle|\mathbf{X}_p|^2\rangle - 1)$ is also drawn. No parameters were adjusted.

MD results of [30], equation (28) is enough and it will be used in the equivalent form

$$\mathbf{X}_p = \frac{b_0}{M}\sum_{n=1}^{M-1}\left\{\left[\sum_{k=n+1}^{M}\cos\left(\frac{p\pi(k-1)}{M-1}\right)\right] - \frac{1}{2}(-1)^p\right\}\mathbf{b}_n. \tag{29}$$

The above equation allows one to express the modulus $\langle|\mathbf{X}_p|^2\rangle$ in terms of the bond–bond static correlations $\langle\mathbf{b}_m \cdot \mathbf{b}_{m+k}\rangle$ by considering, in particular, the expression given by the HM model equation (18). Figure 5 shows that the predictions of the HM model are in good agreement with the MD results for $M = 192$ from [30]. Note that $M = 192$ is well above the entanglement length, which is roughly $N_e \sim 32$ [19].

5. Conclusion

We have shown that excluded-volume effects on single-chain statics may be introduced by analytic corrections to the Rouse results. The final expressions do not depend on free parameters. They exhibit excellent agreement with the molecular-dynamics simulations of *unentangled* polymer melts with chain length in the range $3 \leqslant M \leqslant 30$. Preliminary results for entangled polymer melts are encouraging.

Acknowledgment

Luca Larini is warmly thanked for many helpful discussions.

References

[1] Rouse P E 1953 *J. Chem. Phys.* **21** 1272
[2] Ferry J D 1980 *Viscoelastic Properties of Polymers* 3rd edn (New York: Wiley)
[3] Doi M and Edwards S F 1986 *The Theory of Polymer Dynamics* (Oxford: Clarendon)
[4] Strobl G 1997 *The Physics of Polymers* (New York: Springer)
[5] Verdier P H 1966 *J. Chem. Phys.* **45** 2118
[6] Orwoll R A and Stockmayer W H 1969 *Adv. Chem. Phys.* **15** 305
[7] Verdier P H 1969 *J. Chem. Phys.* **52** 5512
[8] Lin Y-H 2003 *Polymer Viscoelasticity* (Singapore: World Scientific)

[9] Lodge T P, Ritstein N A and Prager S 1999 *Adv. Chem. Phys.* **79** 1
[10] Paul W, Smith G D, Yoon D Y, Farago B, Rathgeber S, Zirkel A, Willner L and Richter D 1998 *Phys. Rev. Lett.* **80** 2346
[11] Doxastakis M, Theodorou D N, Fytas G, Kremer F, Faller R, Müller-Plathe F and Hadjichristidis N 2003 *J. Chem. Phys.* **119** 6883
[12] Pearson D S, Fetters L J, Greassley W W, Ver Strate G and von Meerwall E 1994 *Macromolecules* **27** 711
[13] Guenza M 2002 *Phys. Rev. Lett.* **88** 025901
[14] Binder K, Baschnagel J and Paul W 2003 *Prog. Polym. Sci.* **28** 115
[15] Okun K, Wolfgardt M, Baschnagel J and Binder K 1997 *Macromolecules* **30** 3075
[16] Paul W and Smith G D 2004 *Rep. Prog. Phys.* **67** 1117
[17] Bennemann C, Baschnagel J, Paul W and Binder K 1999 *Comput. Theor. Polym. Sci.* **9** 217
[18] Padding J T and Briels W J 2001 *J. Chem. Phys.* **115** 2846
[19] Baschnagel J and Varnik F 2005 *J. Phys.: Condens. Matter* **17** R851
[20] Muthukumar M and Edwards S F 1981 *J. Chem. Phys.* **76** 2720
[21] Barbieri A, Campani E, Capaccioli S and Leporini D 2004 *J. Chem. Phys.* **120** 437
[22] Eyring H 1932 *Phys. Rev.* **39** 746
Wall F T 1943 *J. Chem. Phys.* **11** 67
[23] Kuhn H 1947 *J. Chem. Phys.* **15** 843
[24] Flory P J 1953 *Principles of Polymer Chemistry* (New York: Cornell University Press)
[25] Grosberg A Yu and Khokhlov A R 1994 *Statistical Physics of Macromolecules* (New York: AIP)
[26] Andersen H C, Chandler D and Weeks J D 1976 *Adv. Chem. Phys.* **34** 105
[27] Schweitzer K S and Curro J G 1997 *Adv. Chem. Phys.* **98** 1
[28] Honnell K G, Curro J G and Schweitzer K S 1990 *Macromolecules* **23** 3496
[29] Allen M P and Tildesley D J 1987 *Computer Simulation of Liquids* (Oxford: Clarendon)
[30] Smith S W, Hall C K and Freeman B D 1996 *J. Chem. Phys.* **104** 5616